nature communications

Article

https://doi.org/10.1038/s41467-026-69567-x

Asymmetric biomimetic transamination of α-keto phosphonates enabled by chiral pyridoxamines and synergistic solvent

Received: 30 September 2025

Accepted: 5 February 2026

Published online: 14 February 2026

Check for updates

Dongchen Cai[1,3], Longjie Huang[1,3], Zhuochuan Wang[1], Siqi Liu[1] ✉, Xiao Xiao[1] ✉ & Baoguo Zhao[1,2] ✉

Chiral α-aminophosphonate derivatives are recognized as valuable compounds in both medicine and organic chemistry. Biomimetic transamination of α-keto phosphonates represents one of the most efficient strategies for accessing these pharmaceutically relevant molecules. However, establishing a general amine-transfer platform that directly delivers N-unprotected chiral α-aminophosphonates remains challenging. We report an asymmetric transamination of α-keto phosphonates catalyzed by a chiral pyridoxamine catalyst, which efficiently affords a diverse range of chiral α-aminophosphonates with up to 86% yield and 98% ee. This methodology provides a straightforward approach to biologically active α-aminophosphonic acid derivatives. Mechanistic studies, supported by DFT calculations, reveal that trifluoroethanol plays a critical role in determining the enantioselectivity and stabilizing the transition states of the rate-limiting step.

The synthesis of chiral primary amines from ketones is a highly valued transformation, given the significance of the amine products and the ready availability and low cost of the ketone substrates (Fig. 1a)[1–3]. Synthetic chemists have utilized the versatile reactivity of imines, such as reduction[4,5], nucleophilic addition[6–11], and 1,3-hydrogen shift[12–21], to access chiral primary amines after deprotection. In nature, transamination of carbonyl compounds, enabled by transaminases via two 1,3-proton shift processes, represents an attractive strategy, as it directly yields N-unprotected chiral amines[22–24]. This approach avoids the condensation, protection, and deprotection steps required in conventional chemical routes. Thus, enzymatic transamination has been extensively studied since the 1950s[25–28]. Today, the enzymatic synthesis of chiral amines catalyzed by transaminases, particularly ω-transaminases (ω-TAs), has been industrialized and successfully applied in the production of various pharmaceuticals[29,30]. Although enzymatic transamination has emerged as a powerful tool for asymmetric synthesis of chiral amines, biomimetic transamination has also attracted considerable interest as a promising approach for chiral amine synthesis[12–21,31–38]. By emulating the structural and mechanistic features of transaminase enzymes, biomimetic catalysts not only retain key aspects of enzymatic efficiency but also benefit from the flexibility and tunability of small-molecule systems, enabling mild and enantioselective synthesis of diverse amines[39–41]. Our group has employed chiral pyridoxamines (**1**), biomimetic catalysts that mimic the structure and function of vitamin B_6-dependent transaminases[42], to achieve the asymmetric transamination of α-keto acids[43,44] and α-keto amides[45]. This platform creates opportunities to develop new transformations by leveraging the unique structural and electronic features of these biomimetic pyridoxamine catalysts.

Chiral α-aminophosphonates stand as an important class of organophosphorus compounds with broad relevance in medicinal and synthetic chemistry[46–49]. Their unique structural and electronic properties enable diverse biological activities, including antibacterial fosfomycin derivative Alafosfalin (hFPPs)[50], the inhibitor of the human farnesyl pyrophosphate synthase[51], imidazoline I_2 receptors (I_2-IRs) ligand in Alzheimer's disease therapy[52], and the inhibitor of matrix

[1]The Education Ministry Key Lab of Resource Chemistry, Shanghai Frontiers Science Center of Biomimetic Catalysis, Shanghai Normal University, Shanghai, China. [2]State Key Laboratory of Synergistic Chem-Bio Synthesis, Shanghai Key Laboratory for Molecular Engineering of Chiral Drugs, School of Chemistry and Chemical Engineering, Shanghai Jiao Tong University, Shanghai, China. [3]These authors contributed equally: Dongchen Cai, Longjie Huang. ✉e-mail: liusq@shnu.edu.cn; xxiao1207@shnu.edu.cn; zhaobg2006@sjtu.edu.cn

https://doi.org/10.1038/s41467-026-69567-x

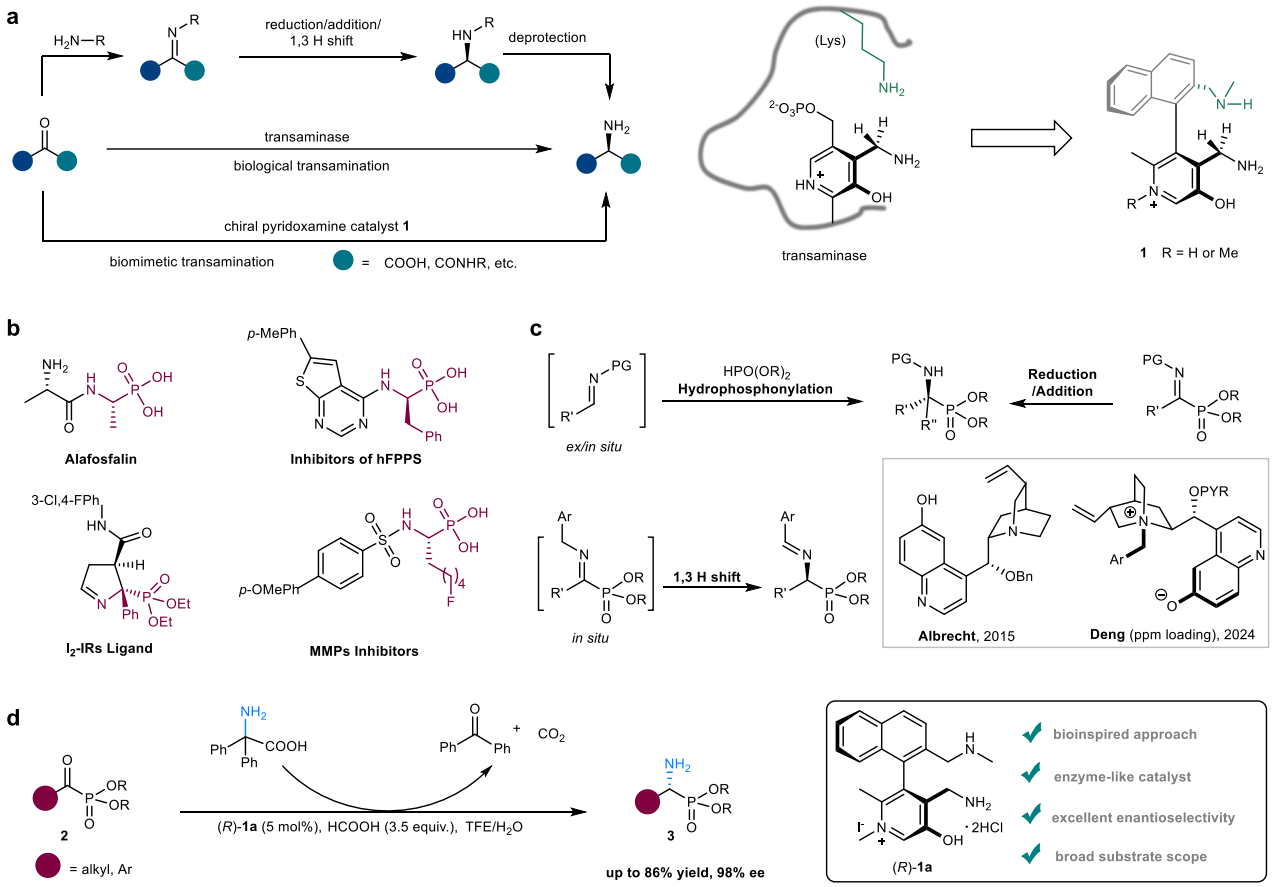

Fig. 1 | Asymmetric biomimetic transamination of α-keto phosphonates enabled by chiral pyridoxamine catalysts. a Different approaches to N-unprotected chiral amines from ketone compounds and the transaminase-inspired chiral pyridoxamine catalysts. **b** Drug-like α-aminophosphonic acid compounds. **c** Representative approaches to N-protected chiral α-aminophosphonates. **d** This work: biomimetic transamination of α-keto phosphonates. PG protecting groups, PYR diphenylpyrimidine, TFE trifluoroethanol.

metalloproteinases (MMPs)[53] (Fig. 1b). Given their pharmacological potential, structural versatility, and synthetic adaptability, a variety of synthetic strategies have been developed for the preparation of chiral α-aminophosphonates[54–56]. Among these, one of the most classical and widely utilized methods is the hydrophosphonylation[57,58], represented by the Kabachnik–Fields reaction[59–61] and Pudovik reaction[62–65]. In addition, chiral α-aminophosphonates also can be efficiently accessed via asymmetric hydrogenation[66,67] or nucleophilic addition[68,69] of iminophosphonates (Fig. 1c, above). In recent years, significant efforts have been directed toward the development of organocatalyzed enantioselective 1,3-proton shift of Schiff bases[70,71], a transformation that mimics the mechanism of biological half-transamination (Fig. 1c, below)[15,42,72]. In 2015, Albrecht and coworkers demonstrated this approach using a cupreine-derived catalyst to facilitate the 1,3-proton shift of in situ generated α-iminophosphonates (from α-ketophosphonates and benzylamines), yielding chiral α-aminophosphonates with excellent enantioselectivity[70]. More recently, Deng's group reported a related strategy employing a betaine-derived quaternary ammonium salt catalyst, which exhibited remarkable efficiency and broad substrate compatibility (Fig. 1c, box)[71]. Despite being the most efficient approach to chiral α-aminophosphonates, enzymatic transamination has rarely been applied to non-proteinogenic α-keto phosphonates, likely due to the inherent substrate specificity of enzymes. Biomimetic asymmetric transamination offers a promising alternative for synthesizing unnatural chiral α-aminophosphonates. However, a general and efficient method for directly accessing N-unprotected derivatives remains scarce[65]. Herein, we report a chiral pyridoxamine-catalyzed biomimetic transamination of α-keto phosphonates that affords structurally diverse chiral α-aminophosphonates in up to 86% yield and 98% ee (Fig. 1d). Mechanistic studies reveal that both the catalyst structure and the solvent microenvironment play decisive roles in controlling the stereoselectivity.

Results

Optimization of reaction conditions

The transamination of α-keto phosphonate **2a** was initially conducted with diphenylglycine (**4a**) as the nitrogen donor and chiral pyridoxamine **1a** as the catalyst at 20 °C (Table 1). The effects of the solvent, ester group, additive, amino donor, and catalyst structure were systematically investigated. Solvent screening revealed that alcohols generally provided higher enantioselectivities, with trifluoroethanol (TFE) proving optimal (entries 1–6, for more details see Supplementary Table S1). Evaluation of the ester group of α-keto phosphonates suggests that both methyl ester and isopropyl ester are suitable for this reaction (Supplementary Table S1, entries 7–10 and 31). Various additives were examined, such as Brønsted acids (Table 1, entries 7–12) and buffer systems (e.g., NaOAc/AcOH, Supplementary Table S1, entries 26 and 27). Among the additives tested, HCOOH markedly accelerated the transamination, affording the product in 83% yield with 97% ee (Table 1, entry 12). In contrast, stronger acids such as CF_3COOH (Table 1, entry 7) or bases like NaOAc (Table 1, entry 9) led to significant

https://doi.org/10.1038/s41467-026-69567-x

Table 1 | Reaction conditions optimization[a]

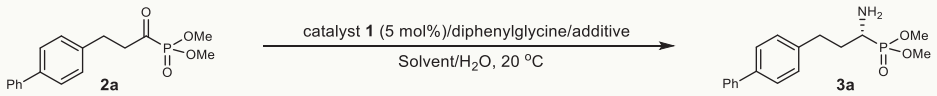

entry	catalyst	solvent	additive	yield (%)[b]	ee(%)[c]	entry	catalyst	solvent	additive	yield (%)[b]	ee(%)[c]
1	**1a**	THF	--	31	43	10	**1a**	TFE	AcOH	70	94
2	**1a**	CH_3CN	--	34	73	11[d]	**1a**	TFE	AcOH	79	96
3	**1a**	DCM	--	n.r.	--	12[d]	**1a**	TFE	HCO_2H	83	97
4	**1a**	EtOH	--	17	87	13[d]	**1b**	TFE	HCO_2H	76	96
5	**1a**	TFE	--	44	93	14[d]	**1c**	TFE	HCO_2H	77	96
6	**1a**	HFIP	--	20	92	15[d]	**1d**	TFE	HCO_2H	83	96
7	**1a**	TFE	CF_3CO_2H	n.r.	--	16[d]	**1e**	TFE	HCO_2H	72	−96
8	**1a**	TFE	KH_2PO_4	66	93	17[d]	**1f**	TFE	HCO_2H	6	45
9	**1a**	TFE	NaOAc	16	89	18[d]	**1g**	TFE	HCO_2H	10	52

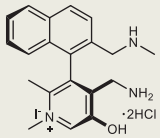
(*R*)-**1a**

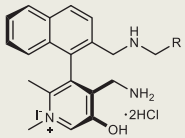
(*R*)-**1b**, R = CH_3
(*R*)-**1c**, R = Ph

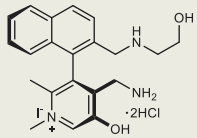
(*R*)-**1d**

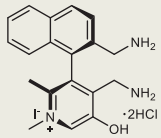
(*S*)-**1e**

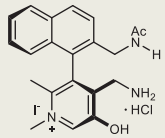
(*R*)-**1f**

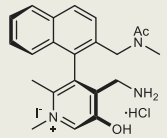
(*R*)-**1g**

Ph phenyl, *Me* Methyl, *Ac* acetyl, *THF* tetrahydrofuran, *DCM* dichloromethane, *TFE* trifluoroethanol, *HFIP* hexafluoroisopropanol.

[a]All the reactions were carried out with α-keto phosphonate **2a** (31.8 mg, 0.1 mmol), diphenylglycine (**4a**) (22.7 mg, 0.1 mmol for entries 1–6; 45.4 mg, 0.2 mmol for entries 7–18), catalyst **1** (0.005 mmol) and additive (0.1 mmol) in solvent/H_2O (0.34 mL/0.06 mL) at 20 °C for 48 h unless otherwise stated.

[b]Isolated yield.

[c]The ee values were determined by HPLC analysis.

[d]Additive (0.35 mmol) and TFE/H_2O (0.51 mL/0.09 mL) were used at 20 °C for 72 h.

decreases in both yield and enantioselectivity. These results suggest that this biomimetic transamination operates optimally under neutral to weakly acidic conditions, which is consistent with the behavior of biological transamination systems. Several alternative amino donors, including *N*,*N*-dimethylglycine (**4b**), methylphenylglycine (**4c**), phenylalanine (**4d**), and benzylamine (**4e**), all afforded <5% yield under the optimized conditions (Supplementary Table S1, entries 32–35). These donors likely fail to promote the essential pyridoxal-to-pyridoxamine conversion required for the catalytic cycle[44,45], whereas diphenylglycine readily undergoes decarboxylation to efficiently convert the pyridoxal to the pyridoxamine catalyst. Catalyst structure has a vital impact on the reactivity and enantioselectivity of this transamination (Table 1, entries 13–18). Catalyst **1a**-**e** bearing an amine side chain all perform well for the transamination in terms of enantioselectivity (Table 1, entries 13–16), implying that the OH group in pyridoxamine **1d** likely doesn't participate in the catalysis via hydrogen bonding (Table 1, entry 15). Catalyst **1e**, which has a primary amine side chain, showed slightly reduced reactivity (Table 1, entry 16). In contrast, catalysts **1f** and **1g**, featuring amide side chains, exhibited a dramatic decrease in both yield and enantiomeric excess (Table 1, entries 17 and 18). These results highlight that the basicity of the amine side chain is crucial for efficient transamination, thereby rendering a secondary amine indispensable for catalysis. Although α-ketophosphonates can act as acylating agents due to the good leaving ability of the phosphonate group, no such side products were observed under our optimized conditions, likely because the acidic environment effectively suppresses this pathway.

Substrate scope study

Under the optimized reaction conditions, substrate scope of the transamination was investigated (Fig. 2). Benzyl and phenethyl substituted α-keto phosphonates all proceeded the amino transfer in the presence of pyridoxamine catalyst **1a** to produce α-amino phosphonates **3b**-**d** in excellent enantioselectivity. Substituents on arylethyl were then examined (for **3e**-**n**). Both electron-donating groups (for **3e, 3f, 3g**, and **3n**) and electron-deficient groups (for **3h**-**m**) generally gave moderate to high reactivity with 92-97% ee. Notably, in contrast with methyl phosphonate, isopropyl phosphonate produced the corresponding chiral α-amino phosphonates with significantly enhanced yields (**3f** *vs* **3g** and **3h** *vs* **3i**). In addition, naphthylethyl (**3q**) and thiophenethyl (**3r**) α-amino phosphonates were respectively obtained in 96% ee with good to high yields. Aliphatic chain substituted α-keto phosphonates underwent the transamination smoothly, delivering a wide range of aliphatic α-amino phosphonates **3t**-**af** in 66-86% yields and 85-98% ee. Various functional groups, such as hetero-atom (as in **3u** and **3ac**), ester (as in **3v** and **3z**), double bond (as in **3aa**), triple bond (as in **3ab**) and alicyclic substituent (as in **3ad**) were all well tolerated. The biomimetic transamination could be also applied to α-keto phosphonates containing complicated moieties. For example, citronellal- and deoxycholic acid-derived α-aminophosphonate **3ae** and **3af** were, respectively, obtained in good yields with high diastereomeric ratios by this transamination. Biologically active molecule (androgen receptor antagonist)[73]-tethered α-amino phosphonate **3ag** was delivered with 68% yield and 90% ee. More importantly, aromatic α-keto phosphonate, a challenging substrate for transamination, was able to produce the desired product **3ah**, albeit with moderate yield and enantioselectivty. Among these products, several chiral aminophosphonates corresponding to natural amino acids, such as **3b** (Phe), **3c** (Tyr), **3t** (Ala), **3u** (Met), and **3v** (Glu), were successfully obtained, demonstrating the method's broad applicability to the synthesis of chiral aminophosphonic acid analogs of proteinogenic amino acids. Unfortunately, Ile- and Val-derived α-keto phosphonates are not effective substrates for the asymmetric transamination, likely due to the steric effect of the β-substituents. The biomimetic reaction completes two half-transamination steps, thereby mimicking the full catalytic cycle of biological transamination[22–24], and directly furnishes a broad range of chiral N-unprotected α-aminophosphonates without requiring any additional hydrolytic manipulation. Taken together, this reaction establishes an alternative platform to the previously reported enantioselective 1,3-proton-shift reactions of Schiff bases[70,71], further expanding the accessible methodological scope for constructing chiral α-aminophosphonates.

Synthetic applications of α-aminophosphonates

The synthetic utility of the transamination was tentatively demonstrated (Fig. 3). The scaled-up reaction was investigated using the (*S*)-**1a** catalyzed transamination of 3.0 mmol of α-ketophosphonate **2a**, affording (*S*)-α-aminophosphonate **3a** in 80% yield and 97% ee, which are also identical to those obtained in the reaction in a small scale (83% yield and 97% ee), demonstrating good scalability for this process. Hydrolysis of (*S*)-**3a** gave chiral improving- aminophosphoric acid **5** in a 96% yield (Fig. 3a). The transamination can also be applied to efficient synthesis of bioactive molecules, such as MMPs inhibitor **8** (Fig. 3b). Transamination of 6-fluorohexanoyl phosphonate (**2ai**) under biomimetic standard conditions afforded chiral α-aminophosphonate **3ai** in 71% yield with 96% ee. Subsequent protection of the NH_2 group using sulfonyl chloride **6** yielded compound **7** in 75% yield while maintaining 95% ee. Hydrolysis of this intermediate delivered the MMPs inhibitor **8**. In contrast, the previous synthetic route started from 6-tetrahydropyranyl-protected 1,6-hexanediol (**9**) and required seven steps, including a chiral resolution, to furnish the corresponding N-protected α-amino phosphonate (**8**) in a mere 4% overall yield[53] (Fig. 3b). In addition, this transamination also can be employed to the rapid synthesis of the enantiomeric analog (**12**) of proteasome inhibitor Ixazomib—a drug approved for the treatment of multiple myeloma (MM)[74]. α-Aminophosphonate **3aj**, which was obtained from **2aj** with 60% yield and 92% ee via catalyst (*S*)-**1a**, was condensed with (2,5-dichlorobenzoyl)glycine (**10**) followed by hydrolysis with TMSBr to produce chiral dipeptide phosphoric acid **12** with 92% ee (Fig. 3c).

Mechanistic study

The reaction follows a typical pyridoxamine catalyzed transamination mechanism[42,72,75], which mimics the two half reactions of enzymatic transamination[43]. The first half-reaction (from α-keto phosphonate **2** to α-amino phosphonate **3**) involves 1,3-proton shift of Schiff base **13** formed between α-keto phosphonate **2** and chiral pyridoxamine (*R*)-**1a**, which is promoted by the intramolecular amine side chain of catalyst[43,44]. The second half-reaction transfers the amine group of diphenyl glycine (**4a**) to internal imine **16**, regenerating chiral pyridoxamine (*R*)-**1a** via the isomerization between Schiff bases **17** and **19** (Fig. 4). Although the internal ammonium species, such as intermediate **14** or **18**, could in principle act as a proton donor for the 1,3-proton shift, in a reaction system containing multiple proton sources (HCOOH, CF_3CH_2OH and H_2O), proton transfer mediated by external proton donors or via a proton-shuttle pathway also represents a plausible mechanism.

Density functional theory (DFT) calculations were performed to elucidate the detailed mechanism of transamination of α-keto phosphonate (**2a**) to chiral α-aminophosphonate (**3a**) and to investigate the origin of chiral induction. The potential energy surface (PES) for the step of the condensation between the **2a** and (*R*)-**1a** is illustrated in Fig. 5. The reaction initiates with the nucleophilic attack of the amine group of pyridoxamine (*R*)-**1a** onto α-keto phosphonate **2a**. This initial step proceeds via transition state **TS1** ($\Delta G^{\ddagger}$ = 15.2 kcal/mol) to generate intermediate **M1**. Assisted by a formic acid-mediated hydrogen-bonding network, a proton is transferred from N1 to O1 through **TS2** to form intermediate **M2**. Subsequently, **M2** undergoes a ligand exchange wherein a formic acid molecule dissociates as a formate ion enters, coordinating with the phenolic hydroxyl group to generate **M3**. This is followed by an intermolecular proton transfer from the phenolic

https://doi.org/10.1038/s41467-026-69567-x

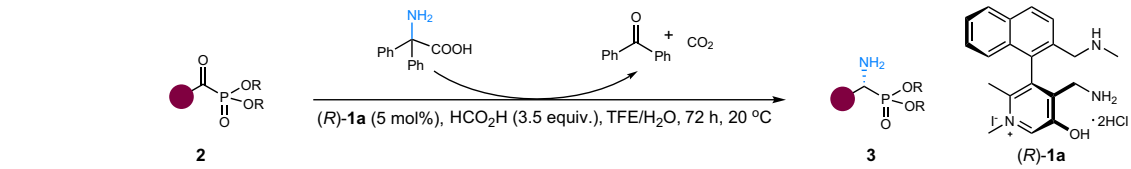

Substrate scope[a]

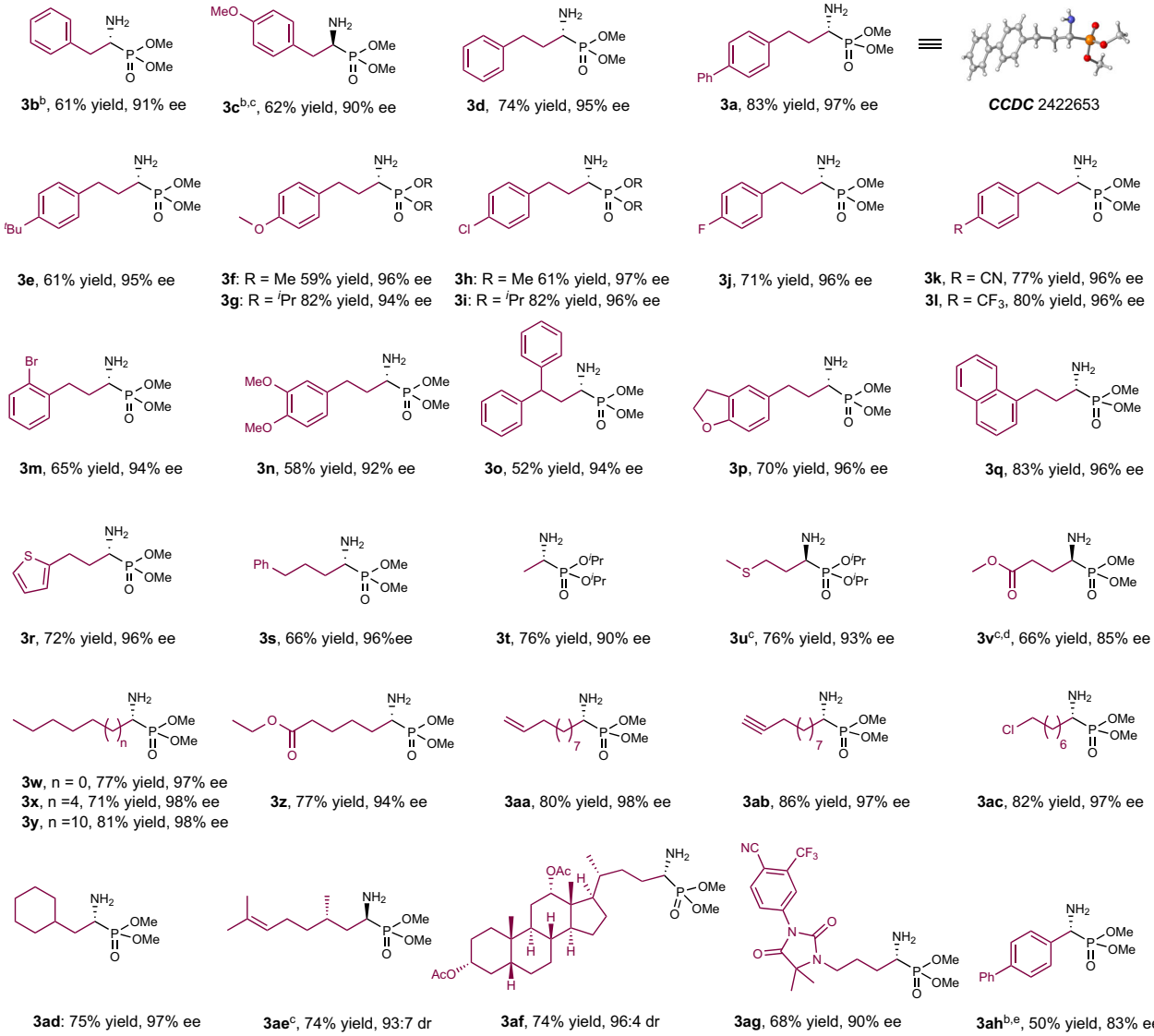

Fig. 2 | Substrate scope study. [a]All the reactions were carried out with α-keto phosphonate **2** (0.1 mmol), diphenylglycine (**4a**) (45.4 mg, 0.2 mmol), catalyst (*R*)−**1a** (2.6 mg, 0.005 mmol) and HCO_2H (16.1 mg, 0.35 mmol) in TFE/H_2O (0.51 mL/0.09 mL) at 20 °C for 72 h unless otherwise stated. [b]10 mol% catalyst loading (5.2 mg, 0.01 mmol) was used. [c]Catalyst (*S*)−**1a** instead of catalyst (*R*)−**1a**. [d]Product **3 v** was isolated as its lactam. [e]Catalyst (*R*)−**1c** (0.01 mmol) instead of catalyst (*R*)-**1a**. Yield: isolated yield based on α-keto phosphonate **2**. The absolute configuration of product **3a** has been determined as *R* by the X-ray analysis and those of **3b**-**3ah** were tentatively assigned by analogy. Ph phenyl, Me Methyl, *i*Pr isopropyl.

hydroxyl group to the formate species via **TS3**. This stage generates intermediate **M4**, which undergoes C1−O1 bond cleavage and the elimination of a water molecule via **TS4** to afford intermediate **M5**. A subsequent proton transfer from N2 to the formate ion proceeds via **TS5**, generating intermediate **M6** (Fig. 5b). The entry of a TFE molecule into the system facilitates hydrogen bonding interaction with the side chain N2−H group, leading to the formation of intermediate **M7**. Subsequently, the benzylic C2−H undergoes deprotonation by the side-chain amine through **TS6** ($\Delta G^{\ddagger}$ = 14.4 kcal/mol) to produce intermediate **M8**. A stereoselective protonation step occurs via **TS7R** ($\Delta G^{\ddagger}$ = 19.7 kcal/mol), furnishing the chiral intermediate **M9R** and ultimately the (*R*)- product. In contrast, the competing transition state **TS7S** is energetically unfavorable, characterized by a significantly higher barrier ($\Delta G^{\ddagger}$ = 25.1 kcal/mol). Geometric analysis reveals that the N−H···O and O−H···O hydrogen bonds are markedly shorter in **TS7R** than in **TS7S**. These shorter distances indicate that the hydrogen-bonding network provides superior stabilization in **TS7R**, thereby lowering its activation barrier relative to **TS7S**. These findings clearly indicate a strong kinetic preference for the *R*-configurational pathway. Further transformation, including intramolecular cyclization and the

https://doi.org/10.1038/s41467-026-69567-x

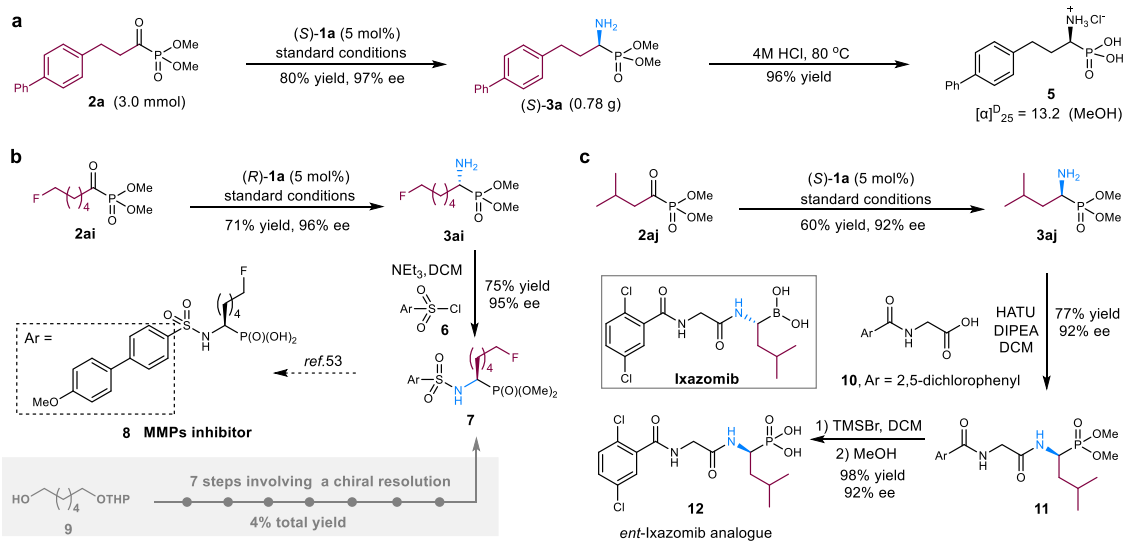

Fig. 3 | Derivatization of α-aminophosphonates. a Scaled-up transamination and hydrolysis of chiral α-aminophosphonate **3a**. **b** Biomimetic synthesis of biologically active molecule **8**. **c** Biomimetic synthesis of drug-like compound **12**. THP tetrahydropyranyl, HATU 2-(7-Azabenzotriazol-1-yl)-N,N,N′,N′-tetramethyluronium hexafluorophosphonate, DIPEA diisopropylethylamine, TMSBr trimethylsilyl bromide.

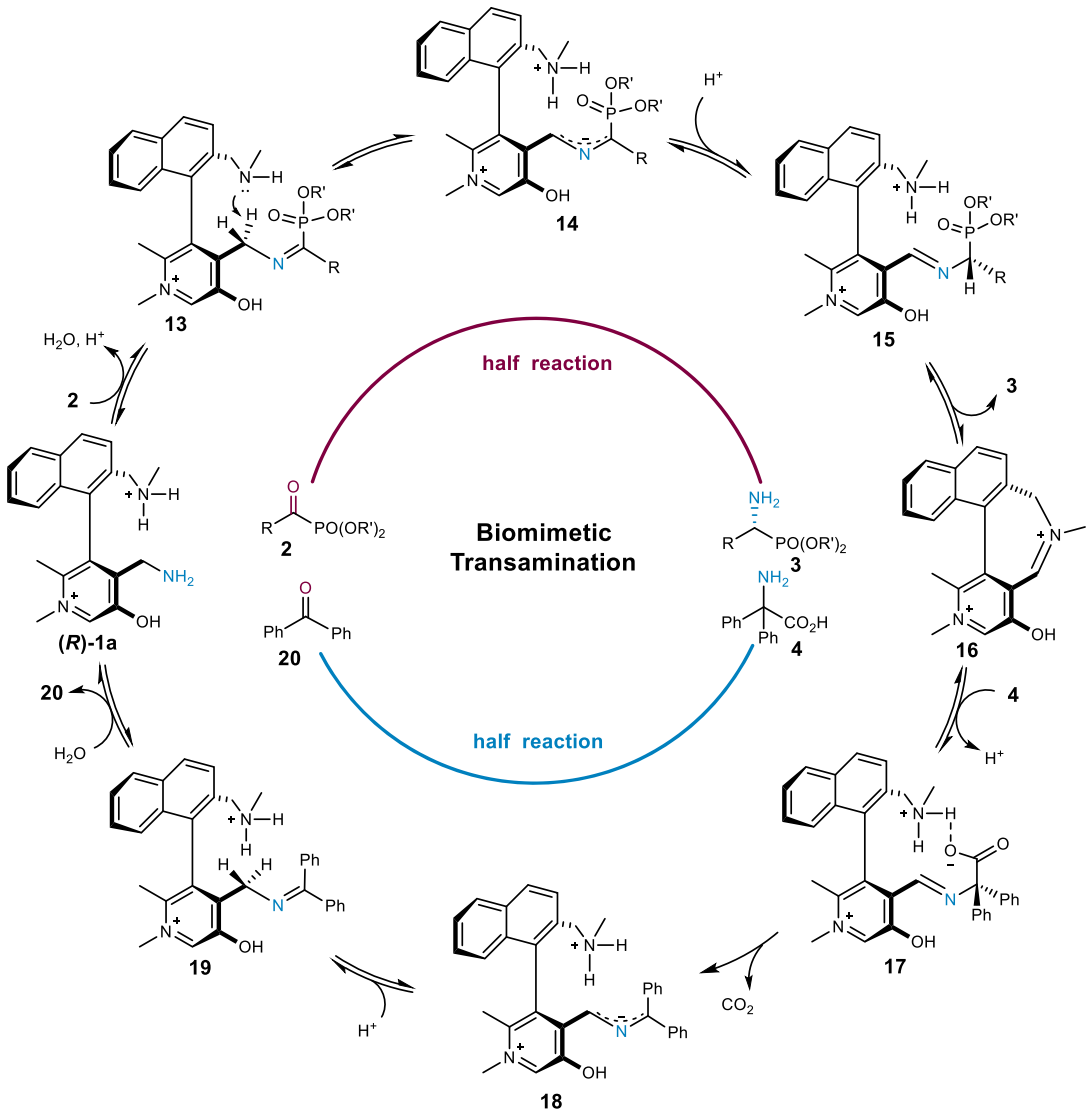

Fig. 4 | Proposed mechanism for transamination of α-keto phosphonates. For clarity, the iodide and chloride anions of the catalyst **1a** are omitted.

https://doi.org/10.1038/s41467-026-69567-x

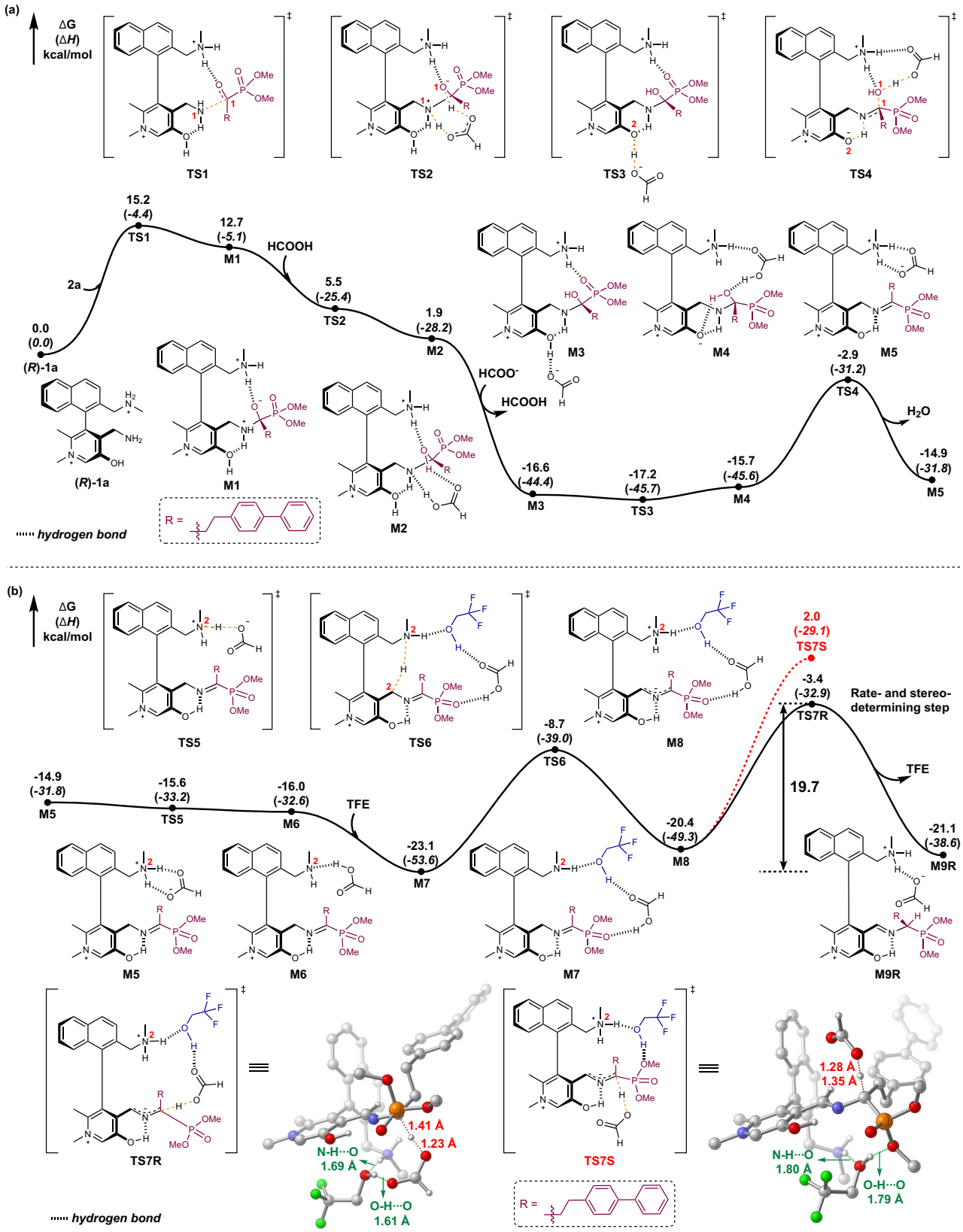

Fig. 5 | Energy profiles and geometries of key transition states for the transamination of α-keto phosphonate. a Energy profile of the condensation step. **b** Energy profile of the proton transfer step and geometries of key transition states. Relative Gibbs free energies are given in kcal/mol. Hydrogen bonds are shown as green dashed lines in the geometries of key transition states. Distances are reported in angstroms (Å). For clarity, the iodide and chloride counterions of catalyst **1a** were excluded from the DFT calculations and are not shown. TFE trifluoroethanol.

https://doi.org/10.1038/s41467-026-69567-x

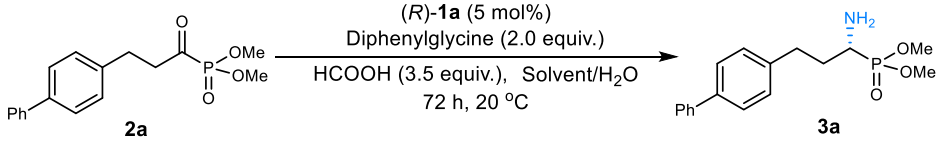

entry[a]	solvent	yield (%)[b]	ee (%)
1	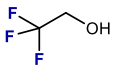	83	97
2	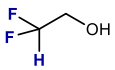	69	93
3	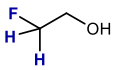	57	88
4	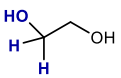	15	82
5	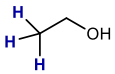	44	78

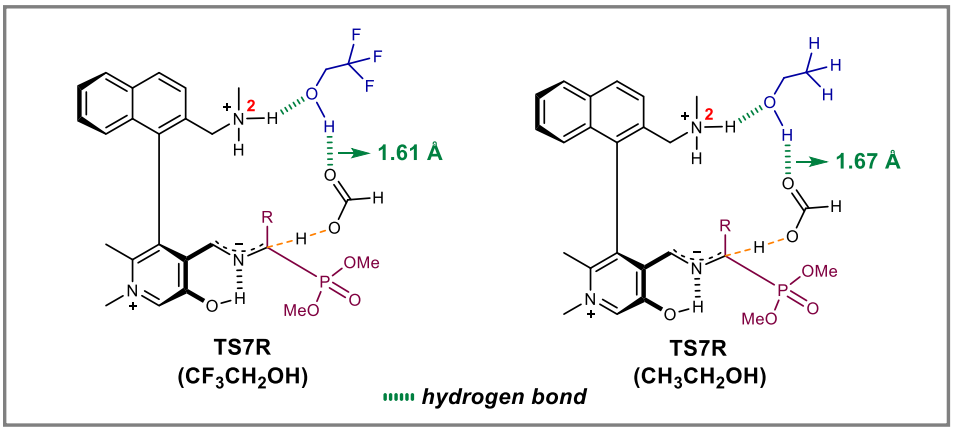

Fig. 6 | Control experiments on alcohol solvents and TS7R transition states in TFE and EtOH. [a]All the reactions were carried out with α-keto phosphonate **2a** (31.8 mg, 0.1 mmol), diphenylglycine (**4a**) (45.4 mg, 0.2 mmol), catalyst (*R*)−**1a** (2.6 mg, 0.005 mmol) and HCO_2H (16.1 mg, 0.35 mmol) in solvent/H_2O (0.51 mL/0.09 mL) at 20 °C for 72 h. [b]Isolated yield.

subsequent release of α-aminophosphonate **3a**, are discussed in the Supplementary Information (Fig. S2). Overall, the computational results identify the protonation of **M8** via **TS7R** is the rate-determining and stereo-determining step for the initial half-transamination.

To further probe the critical role of TFE in the asymmetric 1,3-proton shift process, a series of control experiments were conducted with different alcohol solvents (Fig. 6). Gradual removal of fluorine substituents from the alcohols (from TFE to difluoroethanol and monofluoroethanol) led to a progressive decrease in enantioselectivity (entries 1–3), while ethylene glycol and ethanol afforded substantially lower ee values (entries 4 and 5). These results indicate that the electron-withdrawing effect at the β position of alcohol solvent is crucial for stereochemical induction during the 1,3-proton-shift step. To further rationalize this solvent effect, transition-state calculations were also performed using ethanol as an alternative hydrogen-bonding solvent for **TS7S** and **TS7R**. The calculated difference in Gibbs free energy of activation in ethanol is smaller than that in TFE, capturing the experimentally observed reduction in enantioselectivity (see Supplementary Fig. S3). Moreover, in the **TS7R** transition states in TFE and EtOH (Fig. 6 box), more acidic solvent forms stronger hydrogen-bonding interaction with formate, stabilizing this species and enhancing its proton-donating ability, which in turn improves both enantioselectivity and catalytic activity. In contrast, solvents with weaker acidity display diminished stereocontrol and catalytic efficiency (entries 2–5). Overall, TFE plays a decisive role in enabling both high activity and enantioselectivity, which is critical for the success of this biomimetic transamination.

Discussion

In conclusion, we have developed a highly efficient enantioselective biomimetic transamination of α-keto phosphonates catalyzed by a chiral pyridoxamine derivative with synergistic assistance from the solvent. This method provides direct access to a broad range of biologically active and synthetically valuable chiral α-aminophosphonates in good to excellent yields and with up to 98% ee under mild conditions, highlighting the potential of vitamin B_6-inspired catalysts in asymmetric

synthesis. The strategy features direct transfer of an unprotected amino group, high atom economy, broad substrate scope, and compatibility with complex molecular architectures. Mechanistic studies, supported by DFT calculations, reveal the origin of stereocontrol and identify the rate-determining step of biomimetic transamination. In addition, the solvent environment, exemplified by the decisive role of TFE, was found to cooperate with the catalyst in stabilizing key transition states, thereby contributing to the high enantioselectivity and reflecting the cooperative catalysis principles inherent to enzymatic systems.

Methods

General procedure for the asymmetric transamination

To a 5 mL vial equipped with a magnetic stirrer bar was added **2** (0.10 mmol), (*R*)-**1a** (0.0026 g, 0.005 mmol), diphenylglycine (**4a)** (0.0454 g, 0.2 mmol), trifluoroethanol (TFE, 0.51 mL), H_2O (0.09 mL) and HCO_2H (0.0161 g, 0.35 mmol) under N_2 atmosphere. Upon stirring at 20 °C for 72 h, the reaction mixture was evaporated to remove most of the solvent and submitted to flash column chromatography on silica gel (DCM:MeOH:saturated NH_3 solution in ethanol = 50:1:1) to give product **3**. For some specific substrates, the reaction conditions were slightly changed, the detailed information of which can be found in the Supplementary Information.

Data availability

The authors declare that the data supporting the findings of this study are available within the article and Supplementary Information file, or from the corresponding author upon request. The X-ray crystallographic coordinates for structures reported in this study have been deposited at the Cambridge Crystallographic Data Centre (CCDC), under deposition numbers of CCDC 2422653 [compound (*R*)-**3a** in Supplementary Information Fig. S1]. These data can be obtained free of charge from The Cambridge Crystallographic Data Centre via https://www.ccdc.cam.ac.uk/structures/. Coordinates of the optimized structures are present as source data. Source data are provided with this paper.

References

1. Kroutil, W. et al. Asymmetric preparation of prim-, sec-, and tert-amines employing selected biocatalysts. *Org. Process Res. Dev*. **17**, 751–759 (2013).
2. Yin, Q., Shi, Y., Wang, J. & Zhang, X. Direct catalytic asymmetric synthesis of α-chiral primary amines. *Chem. Soc. Rev*. **49**, 6141–6153 (2020).
3. Yin, Q., Zhang, X., Shi, Y. & Rong, N. Synthesis of chiral primary amines via enantioselective reductive amination: from academia to industry. *Synthesis* **55**, 1053–1068 (2023).
4. Abdine, R. A. A., Hedouin, G., Colobert, F. & Wencel-Delord, J. Metal-catalyzed asymmetric hydrogenation of C═N bonds. *ACS Catal*. **11**, 215–247 (2021).
5. Cabré, A., Verdaguer, X. & Riera, A. Recent advances in the enantioselective synthesis of chiral amines via transition metal-catalyzed asymmetric hydrogenation. *Chem. Rev*. **122**, 269–339 (2022).
6. Wang, J., Liu, X. & Feng, X. Asymmetric Strecker reactions. *Chem. Rev*. **111**, 6947–6983 (2011).
7. Kurono, N. & Ohkuma, T. Catalytic asymmetric cyanation reactions. *ACS Catal*. **6**, 989–1023 (2016).
8. Wu, P., Givskov, M. & Nielsen, T. E. Reactivity and synthetic applications of multicomponent Petasis reactions. *Chem. Rev*. **119**, 11245–11290 (2019).
9. Hou, X. Q. & Du, D. M. Recent advances in squaramide-catalyzed asymmetric Mannich reactions. *Adv. Synth. Catal*. **362**, 4487–4512 (2020).
10. Onyeagusi, C. I. & Malcolmson, S. J. Strategies for the catalytic enantioselective synthesis of α-trifluoromethyl amines. *ACS Catal*. **10**, 12507–12536 (2020).
11. Lupidi, G., Palmieri, A. & Petrini, M. Enantioselective catalyzed synthesis of amino derivatives using electrophilic open-chain N-activated ketimines. *Adv. Synth. Catal*. **363**, 3655–3692 (2021).
12. Willems, J. G. H., de Vries, J. G., Nolte, R. J. M. & Zwanenburg, B. Asymmetric imine isomerisation in the enantioselective synthesis of chiral amines from prochiral ketones. *Tetrahedron Lett*. **36**, 3917–3920 (1995).
13. Knudsen, K. R., Bachmann, S. & Jørgensen, K. A. Catalytic enantioselective transaminiation of α-keto esters: an organic approach to enzymatic reactions. *Chem. Commun*. **20**, 2602–2603 (2003).
14. Han, J. et al. Biomimetic transamination—a metal-free alternative to the reductive amination. Application for generalized preparation of fluorine-containing amines and amino acids. *Curr. Org. Synth*. **8**, 281–294 (2011).
15. Xie, Y., Pan, H., Liu, M., Xiao, X. & Shi, Y. Progress in asymmetric biomimetic transamination of carbonyl compounds. *Chem. Soc. Rev*. **44**, 1740–1748 (2015).
16. Xiao, X., Xie, Y., Su, C., Liu, M. & Shi, Y. Organocatalytic asymmetric biomimetic transamination: from α-keto esters to optically active α-amino acid derivatives. *J. Am. Chem. Soc*. **133**, 12914–12917 (2011).
17. Wu, Y. & Deng, L. Asymmetric synthesis of trifluoromethylated amines via catalytic enantioselective isomerization of imines. *J. Am. Chem. Soc*. **134**, 14334–14337 (2012).
18. Zhou, X., Wu, Y. & Deng, L. Cinchonium betaines as efficient catalysts for asymmetric proton transfer catalysis: The development of a practical enantioselective isomerization of trifluoromethyl imines. *J. Am. Chem. Soc*. **138**, 12297–12302 (2016).
19. Kang, Q.-K., Selvakumar, S. & Maruoka, K. Asymmetric synthesis of α-amino acids by organocatalytic biomimetic transamination. *Org. Lett*. **21**, 2294–2297 (2019).
20. Peng, Q. et al. Biomimetic enantioselective synthesis of β,β-difluoro-α-amino acid derivatives. *Commun. Chem*. **4**, 148 (2021).
21. Mayer, R. J., Kaur, H., Rauscher, S. A. & Moran, J. Mechanistic insight into metal ion-catalyzed transamination. *J. Am. Chem. Soc*. **143**, 19099–19111 (2021).
22. Bender, D. *Transaminases* (Wiley, 1985).
23. Rozzell, J. D. & Bommarius, A. S. Transaminations. in *Enzyme Catalysis in Organic Synthesis* 873–893 (Wiley, 2002).
24. D'Mello, J. P. F. *Amino Acids in Human Nutrition and Health* (CAB International, 2012).
25. Höhne, M. & Bornscheuer, U. T. Application of transaminases. in *Enzyme Catalysis in Organic Synthesis* 779–820 (Wiley, 2012).
26. Zhu, D. & Hua, L. Biocatalytic asymmetric amination of carbonyl functional groups—a synthetic biology approach to organic chemistry. *Biotechnol. J*. **4**, 1420–1431 (2009).
27. Slabu, I., Galman, J. L., Lloyd, R. C. & Turner, N. J. Discovery, engineering, and synthetic application of transaminase biocatalysts. *ACS Catal*. **7**, 8263–8284 (2017).
28. Israr, M., Padhi, S. K., Zhou, Y. & Wu, S. Recent advances in protein engineering and synthetic applications of amino acid transaminases. *ChemCatChem* **17**, e202401952 (2025).
29. Kelly, S. A. et al. Application of ω-transaminases in the pharmaceutical industry. *Chem. Rev*. **118**, 349–367 (2018).
30. Madsen, J. Ø & Woodley, J. M. Considerations for the scale-up of in vitro transaminase-catalyzed asymmetric synthesis of chiral amines. *ChemCatChem* **15**, e202300560 (2023).
31. Kuzuhara, H., Komatsu, T. & Emoto, S. Synthesis of a chiral pyridoxamine analog and nonenzymatic stereoselective transamination. *Tetrahedron Lett*. **19**, 3563–3566 (1978).
32. Ronald Breslow, M. H. & Manfred, L. Selective transamination and optical induction by a β-cyclodextrin-pyridoxamine artificial enzyme. *J. Am. Chem. Soc*. **102**, 421–422 (1980).
33. Zimmerman, S. C. & Breslow, R. Asymmetric synthesis of amino acids by pyridoxamine enzyme analogs utilizing general base-acid catalysis. *J. Am. Chem. Soc*. **106**, 1490–1491 (1984).

34. Kuang, H. & Distefano, M. D. Catalytic enantioselective reductive amination in a host–guest system based on a protein cavity. *J. Am. Chem. Soc.* **120**, 1072–1073 (1998).
35. Kikuchi, J. -i, Zhang, Z.-Y. & Murakami, Y. Enantioselective catalysis by a supramolecular bilayer membrane as an artificial aminotransferase. Stereochemical roles of an *L*-lysine residue and *L*-phenylalanine at the reaction site. *J. Am. Chem. Soc.* **117**, 5383–5384 (1995).
36. Svenson, J., Zheng, N. & Nicholls, I. A. A molecularly imprinted polymer-based synthetic transaminase. *J. Am. Chem. Soc.* **126**, 8554–8560 (2004).
37. Wei, S., Wang, J., Venhuizen, S., Skouta, R. & Breslow, R. Dendrimers in solution can have their remote catalytic groups folded back into the core: enantioselective transaminations by dendritic enzyme mimics-II. *Bioorg. Med. Chem. Lett.* **19**, 5543–5546 (2009).
38. Zhang, S. et al. Bio-inspired enantioselective full transamination using readily available cyclodextrin. *RSC Adv.* **7**, 4203–4208 (2017).
39. Breslow, R. Biomimetic chemistry and artificial enzymes: catalysis by design. *Acc. Chem. Res.* **28**, 146–153 (1995).
40. Marchetti, L. & Levine, M. Biomimetic catalysis. *ACS Catal.* **1**, 1090–1118 (2011).
41. Xiao, X. et al. Biomimetic asymmetric catalysis. *Sci. China Chem.* **66**, 1553–1633 (2023).
42. Xiao, X. & Zhao, B. Vitamin B_6-based biomimetic asymmetric catalysis. *Acc. Chem. Res.* **56**, 1097–1117 (2023).
43. Shi, L. et al. Chiral pyridoxal-catalyzed asymmetric biomimetic transamination of α-keto acids. *Org. Lett.* **17**, 5784–5787 (2015).
44. Liu, Y. E. et al. Enzyme-inspired axially chiral pyridoxamines armed with a cooperative lateral amine chain for enantioselective biomimetic transamination. *J. Am. Chem. Soc.* **138**, 10730–10733 (2016).
45. Cai, W. et al. Asymmetric biomimetic transamination of α-keto amides to peptides. *Nat. Commun.* **12**, 5174 (2021).
46. Kukhar′, V. P. *Aminophosphonic and Aminophosphinic Acids: Chemistry and Biological Activity* (Wiley, 2000).
47. Naydenova, E. D., Todorov, P. T. & Troev, K. D. Recent synthesis of aminophosphonic acids as potential biological importance. *Amino Acids* **38**, 23–30 (2010).
48. Mucha, A., Kafarski, P. & Berlicki Remarkable potential of the α-aminophosphonate/phosphinate structural motif in medicinal chemistry. *J. Med. Chem.* **54**, 5955–5980 (2011).
49. Mayorquín-Torres, M. C., Simoens, A., Bonneure, E. & Stevens, C. V. Synthetic methods for azaheterocyclic phosphonates and their biological activity: an update 2004–2024. *Chem. Rev.* **124**, 7907–7975 (2024).
50. Lejczak, B., Kafarski, P., Sztajer, H. & Mastalerz, P. Antibacterial activity of phosphono dipeptides related to alafosfalin. *J. Med. Chem.* **29**, 2212–2217 (1986).
51. Park, J. et al. Pharmacophore mapping of thienopyrimidine-based monophosphonate (Thp-Mp) inhibitors of the human farnesyl pyrophosphate synthase. *J. Med. Chem.* **60**, 2119–2134 (2017).
52. Bagán, A. et al. Discovery of (3-phenylcarbamoyl-3,4-dihydro-2H-pyrrol-2-yl)phosphonates as imidazoline I_2 receptor ligands with anti-Alzheimer and analgesic properties. *J. Med. Chem.* **68**, 2551–2573 (2025).
53. Beutel, B., Daniliuc, C. G., Riemann, B., Schäfers, M. & Haufe, G. Fluorinated matrix metalloproteinases inhibitors—phosphonate based potential probes for positron emission tomography. *Bioorg. Med. Chem.* **24**, 902–909 (2016).
54. Ma, J.-A. Catalytic asymmetric synthesis of α- and β-amino phosphonic acid derivatives. *Chem. Soc. Rev.* **35**, 630–636 (2006).
55. Ordóñez, M., Viveros-Ceballos, J. L., Cativiela, C. & Sayago, F. J. An update on the stereoselective synthesis of α-aminophosphonic acids and derivatives. *Tetrahedron* **71**, 1745–1784 (2015).
56. Varga, P. R. & Keglevich, G. The last decade of optically active α-aminophosphonates. *Molecules* **28**, 6150 (2023).
57. Maestro, A., de Marigorta, E. M., Palacios, F. & Vicario, J. α-iminophosphonates: useful intermediates for enantioselective synthesis of α-aminophosphonates. *Asian J. Org. Chem.* **9**, 538–548 (2020).
58. Amira, A. et al. Recent advances in the synthesis of α-aminophosphonates: a review. *ChemistrySelect* **6**, 6137–6149 (2021).
59. Cheng, X., Goddard, R., Buth, G. & List, B. Direct catalytic asymmetric three-component Kabachnik–Fields reaction. *Angew. Chem. Int. Ed.* **47**, 5079–5081 (2008).
60. Zhou, X. et al. Enantioselective three-component Kabachnik–Fields reaction catalyzed by chiral scandium(III)–N,N′-dioxide complexes. *Org. Lett.* **11**, 1401–1404 (2009).
61. Dai, Y., Zheng, L., Chakraborty, D., Borhan, B. & Wulff, W. D. Zirconium-catalyzed asymmetric Kabachnik–Fields reactions of aromatic and aliphatic aldehydes. *Chem. Sci.* **12**, 12333–12345 (2021).
62. Joly, G. D. & Jacobsen, E. N. Thiourea-catalyzed enantioselective hydrophosphonylation of imines: Practical access to enantiomerically enriched α-amino phosphonic acids. *J. Am. Chem. Soc.* **126**, 4102–4103 (2004).
63. Nakamura, S. et al. Catalytic enantioselective hydrophosphonylation of ketimines using cinchona alkaloids. *J. Am. Chem. Soc.* **131**, 18240–18241 (2009).
64. Yin, L., Bao, Y., Kumagai, N. & Shibasaki, M. Catalytic asymmetric hydrophosphonylation of ketimines. *J. Am. Chem. Soc.* **135**, 10338–10341 (2013).
65. Yamada, K. et al. Organocatalytic direct enantioselective hydrophosphonylation of N-unsubstituted ketimines for the synthesis of α-aminophosphonates. *ACS Catal.* **13**, 3158–3163 (2023).
66. Zhang, J., Li, Y., Wang, Z. & Ding, K. Asymmetric hydrogenation of α- and β-enamido phosphonates: Rhodium(I)/monodentate phosphoramidite catalyst. *Angew. Chem. Int. Ed.* **50**, 11743–11747 (2011).
67. Yan, Z., Wu, B., Gao, X., Chen, M.-W. & Zhou, Y.-G. Enantioselective synthesis of α-amino phosphonates via pd-catalyzed asymmetric hydrogenation. *Org. Lett.* **18**, 692–695 (2016).
68. Liu, Y.-J., Li, J.-S., Nie, J. & Ma, J.-A. Organocatalytic asymmetric decarboxylative mannich reaction of β-keto acids with cyclic α-ketiminophosphonates: access to quaternary α-aminophosphonates. *Org. Lett.* **20**, 3643–3646 (2018).
69. Maestro, A., Martinez de Marigorta, E., Palacios, F. & Vicario, J. Enantioselective α-aminophosphonate functionalization of indole ring through an organocatalyzed Friedel–Crafts reaction. *J. Org. Chem.* **84**, 1094–1102 (2019).
70. Kowalczyk, D. & Albrecht An organocatalytic biomimetic approach to α-aminophosphonates. *Chem. Commun.* **51**, 3981–3984 (2015).
71. Lu, J., Yu, Y., Li, Z., Luo, J. & Deng, L. Practical synthesis of chiral α-aminophosphonates with weak bonding organocatalysis at ppm loading. *J. Am. Chem. Soc.* **146**, 16706–16713 (2024).
72. Liao, R. Z., Ding, W. J., Yu, J. G., Fang, W. H. & Liu, R. Z. Theoretical studies on pyridoxal 5′-phosphate-dependent transamination of α-amino acids. *J. Comput. Chem.* **29**, 1919–1929 (2008).
73. Sexton, K. E. et al. Pantolactams as androgen receptor antagonists for the topical suppression of sebum production. *Bioorg. Med. Chem. Lett.* **21**, 5230–5233 (2011).
74. Moreau, P. et al. Oral ixazomib, lenalidomide, and dexamethasone for multiple myeloma. *N. Engl. J. Med.* **374**, 1621–1634 (2016).
75. Han, L.-L. et al. Biomimetic asymmetric transamination reactions catalyzed by axial pyroxamine organocatalysts: mechanism and origin of stereoselectivity. *Mol. Catal.* **549**, 113514 (2023).

Acknowledgements

We are grateful for the generous financial support from National Key R&D Program of China (2023YFA1506400, B.Z. and X.X.), National Natural Science Foundation of China (NSFC) (22271192, B.Z.; 22471171, X.X. 22403065, S.L.), The Science Fund for Excellent Research Groups (Category A) (T2588102), Shanghai Municipal Science and Technology

Major Project (B.Z.) and the Shanghai Engineering Research Center of Green Energy Chemical Engineering (18DZ2254200, B.Z.).

Author contributions

B.Z. conceived and directed the project and wrote the paper. X.X. co-directed the project and wrote the manuscript. S.L. directed the DFT calculation and wrote the corresponding section in the text. D.C. performed the experiments and wrote most of the supplementary documents. L.H. conducted the DFT calculations and wrote the corresponding section in Supplementary Information. Z.W. conducted the part of synthetic applications.

Competing interests

The authors declare no competing interests.

Additional information

Supplementary information The online version contains supplementary material available at https://doi.org/10.1038/s41467-026-69567-x.

Correspondence and requests for materials should be addressed to Siqi Liu, Xiao Xiao or Baoguo Zhao.

Peer review information *Nature Communications* thanks Jun-An Ma, Javier Vicario and the other anonymous reviewer(s) for their contribution to the peer review of this work. A peer review file is available.